Applied Physics A (2021) 127:660
https://doi.org/10.1007/s00339-021-04819-9

Applied Physics A
Materials Science & Processing

RAPID COMMUNICATIONS

AlGaN-based ternary nitride memristors

Seok Choi[1] · Ha Young Lee[1] · Hee Ju Yun[1] · Byung Joon Choi[1]

Received: 11 June 2021 / Accepted: 3 August 2021

Abstract
Resistive switching memory or memristors have been extensively studied worldwide, driven by perspective applications in nonvolatile memory, processing-in-memory, and neuromorphic computing hardware. Binary oxides are the most prevalent memristive materials; however, non-oxide materials can also exhibit resistive switching. In this study, ternary nitride alloy memristors were fabricated using AlGaN films and were investigated. AlGaN memristors exhibit highly linear and repeatable resistive switching characteristics. Structural and chemical analyses indicate a plausible mechanism of the conduction channel formation in the ternary nitride memristors.

Keywords Resistive switching memory · Memristors · AlGaN · Ternary nitride · Atomic layer deposition

1 Introduction

The rapidly growing demand for information processing is a significant challenge for the big-data era. Alternative computing architecture or energy-efficient brain-inspired computing has been suggested to reduce the effect of "bottleneck" or "memory wall" caused by the frequent data transfer between memory and processing units [1, 2]. Such new computing approaches require nonvolatile memory devices and materials to enable high-throughput, energy-efficient, and area-efficient information processing [3, 4]. Many major memory technologies have been explored so far; resistive switching memories or memristors are considered as strong candidates capable of applications in "processing-in-memory" [5–8]. This is because its operating mechanism of memristors relies on the use of physical phenomena–formation and rupture of conducting channel–to implement the complicated signal transformation [3]. However, the voltage–time dilemma and tradeoff relation between low-energy operation and its variations are current major huddles in practical applications of memristor devices and materials [9–11].

Recently, it was reported that nitride materials can exhibit resistive switching and thus potentially offer desirable properties, including high-speed (switching enabled by pulse width < 100 ps) and low-energy switching (< 10 μA at 50×50 nm^2) [12, 13]. Several nitride-based materials have been studied so far; AlN, Si_3N_4, NiN, CuN, and $HfO_{2-x}N_x$ have been demonstrated that they possess excellent resistive switching behaviors [12–17]. Recently, Guo et al. reported that synaptic device based on AlN memristor could mimic biological synaptic characteristics such as ling-term potentiation and long-term depression, which is essential for neuromorphic computing [18]. Furthermore, nitride memristors can be readily extended to power electronic devices, where nitride compound semiconductors, such as GaN, $Al_xGa_{1-x}N$, and $In_xGa_{1-x}N$, are used as channel materials for high electron mobility transistors (HEMTs) that can provide high speed and voltage to nitride memristors [13, 19].

In this study, an AlGaN memristor was investigated for its potential application in nonvolatile memory to satisfy the requirement of low variation and high linearity. The AlN memristor showed ultrahigh-speed and low-current operation. However, device variation was severe owing to the stochastic nature of Al-rich conduction channel formed in the AlN matrix. It is considered that the atomically dispersed semiconducting GaN into an insulating AlN matrix may significantly reduce the variation in memristor memory cells.

✉ Byung Joon Choi
bjchoi@seoultech.ac.kr

[1] Department of Materials Science and Engineering, Seoul National University of Science and Technology, Seoul 01811, Korea

Published online: 10 August 2021

2 Experimental

AlGaN and AlN films were deposited by atomic layer deposition (ALD) using trimethylaluminum (TMA, $Al(CH_3)_3$), trimethylgaluim (TMG, $Ga(CH_3)_3$), and N_2:H_2 (20:40 SCCM) mixed gas as the metal organic precursors and a plasma reactant gas at a wafer temperature of 350 °C. Figure 1a shows a schematic of the methyl precursor molecules with reactive sites on the surface. To grow the ternary nitride films, a supercycle of AlN and GaN subcycles, a combination of the digital pulsing of AlN and GaN film was used [20–22]. Specifically, a subcycle ratio (AlN: GaN) of 2: 5 was employed for the memristor fabrication.

Rutherford backscattering spectrometry (RBS; 6SDH-2, NEC, USA) and X-ray photoelectron spectroscopy (XPS; PHI 5000 Versa Probe, ULVAC-PHI, Japan) with a monochrome Al Kα (1488.6 keV) source were used to examine the chemical composition and bonding state of AlGaN and AlN films.

The memristors were fabricated with a crossbar structure. The bottom electrode was a 25-nm-thick Pt layer grown by an e-beam evaporator. AlGaN and AlN films of 6–8-nm-thickness were deposited by ALD. Then, the top electrode was sputter-grown with 3-nm-thick TiN and 20-nm-thick evaporated Pt layer. Electrodes were photolithographically patterned using a lift-off method. Figure 1b and c shows schematics of the memristor stack and scanning electron microscopy (SEM, JSM-6700F, JEOL, Japan) image of the memristor with 5×5 μm^2. During the acquisition of electrical data, a quasi-DC voltage sweep was applied to the top electrode with the bottom contact grounded at room temperature. Before displaying reversible switching, the as-prepared memristors required an "electroforming" process. Transmission electron microscopy (TEM, JEM-2100F, JEOL, Japan), combined with energy-dispersive X-ray spectroscopy (EDS), was used to observe the cross-section and elemental mapping of the memristor.

3 Results and discussion

Resistive switching induced by electrical stimuli is presented. Figure 2a and b shows 100 consecutive switching current–voltage (*I–V*) loops (sweep rate was about 10 V/sec) of the Pt/TiN/AlGaN (7 nm)/Pt and Pt/TiN/AlN (6.4 nm)/Pt devices on a linear scale, respectively. The resistive switching is of a bipolar type, meaning the bias voltage of opposite polarity should be applied for a reversible transition between the high-resistance state (HRS) and low-resistance state (LRS). The devices could be transitioned from HRS to LRS (so called SET operation noted as ①) at approximately + 0.5 V. LRS was maintained even the applied voltage was back to 0 V (②). After that, LRS abruptly reversed to HRS (③RESET operation) at about − 0.5 to −0.6 V for both devices by applying a negative voltage sweep, which was also maintained at 0 V (④). Both the devices exhibited excellent repeatability. The device area was relatively large (5 μm × 5 μm) compared to the commercial device dimensions; thus, the ON-current was of the order of milliamperes. Both the devices showed highly linear *I–V* loops, that is, the resistances of HRS and LRS were quite low. Therefore, it appears that highly conducting channels are formed, and their lateral growth/retardation could be responsible for the switching similar to a TaO_x memristor [10].

There was, however, a small but nonnegligible difference observed in the variation of resistance and linearity of resistance states between the two devices. Figure 2c and d shows the resistance–voltage (*R–V*) loops of the first 8 switching cycles from above. In particular, the *R–V* loops of AlGaN device exhibit highly linear and constant resistances, implying that metallic conduction channels without an electrical barrier layer are formed. It is noteworthy that linearity is almost maintained up to the switching voltage with a low variation. Nonlinear *R–V* characteristics with a larger variation were observed even in the LRS of the AlN memristor. It is known that a low variation is highly desirable for synaptic devices as an essential component of neuromorphic

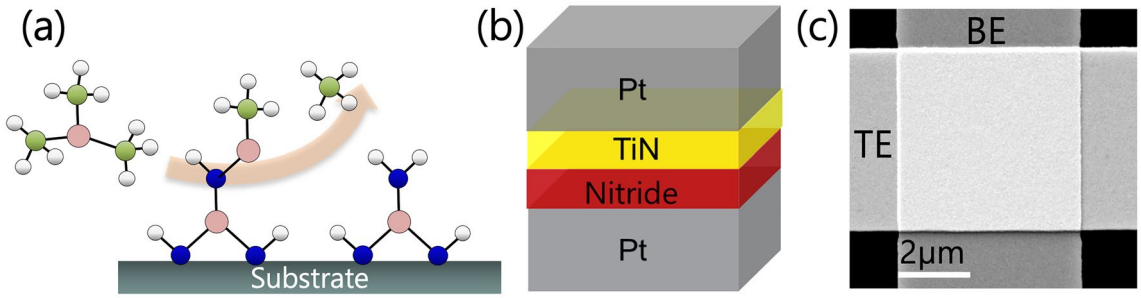

Fig. 1 **a** Schematic of methyl precursor molecules in ALD reaction. **b** Schematic of memristor stack. **c** SEM top-view image of memristor with an area of 5×5 μm^2 (scale bar: 2 μm)

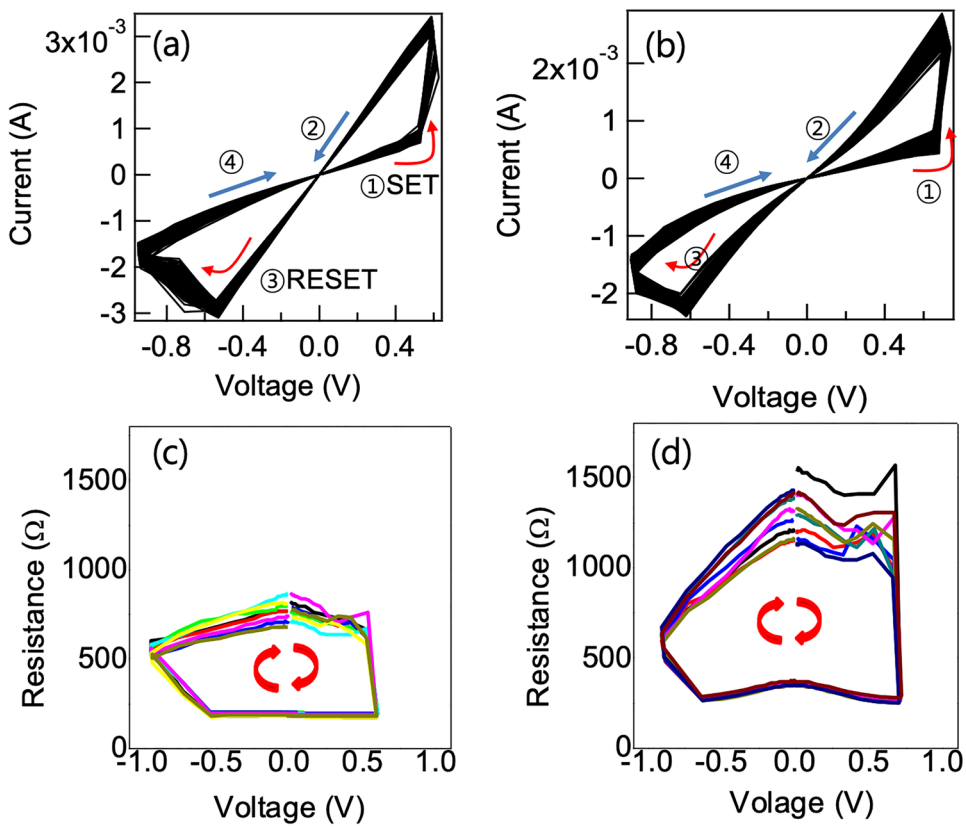

Fig. 2 Repeatable switching *I–V* loops of **a** AlGaN and **b** AlN microdevices and their first 8 switching cycles represented by *R–V* loops in **c** and **d**

computing and resistive switching memory applications [3, 10].

Depth elemental profiles of the devices with AlGaN and AlN were performed by using RBS. As shown in Fig. 3a and b, it was revealed that the devices had $Al_{0.7}Ga_{0.3}$ N (Al:Ga = 34.7:15.3) and stoichiometric AlN (Al:N = 50:50) films. Therefore, to further elucidate the correlation between chemical bonding state in the film and its electrical properties, the current density–electric field (*J–E*) curves of the devices made of various nitride films, including GaN, $Al_{0.7}Ga_{0.3}$ N, $Al_{0.9}Ga_{0.1}$ N, and AlN, are presented in Fig. 4a. The variation in the junction area and film thickness of the devices were taken into consideration from their pristine *I–V* characteristics. The devices with AlN and $Al_{0.9}Ga_{0.1}$ N films had the most insulating nature. However, the device with the GaN film exhibited linear *I–V* characteristics. The device with an ALD-grown GaN film exhibited a resistivity of 790 Ω cm, which is comparable to that of undoped GaN films previously reported in literature, with a wide range of ~ 10^5 to ~ 2×10^{-3} Ω cm for undoped or doped GaN films grown by sputtering or pulsed laser deposition [23, 24]. In the case of the device with $Al_{0.7}Ga_{0.3}$ N film, the *J–E* curve is in between those of GaN and AlN devices but closer to that of AlN. It is well known that band gap energy of $Al_xGa_{1-x}N$ alloys could be tuned as a function of the composition. Band gap energy of AlN (~ 6.1 eV) is much higher than that of GaN (~ 3.5 eV) so that band gap energy of $Al_xGa_{1-x}N$ alloy could be increased with increasing Al content [25]. Such an increase of band gap energy could increase the energy barrier for the electrical conduction, which in turn, reduces the electrical conductivity of the device. Therefore, it is natural that the electrical property of the device with $Al_{0.7}Ga_{0.3}$ N film becomes more insulating than that of the device with GaN film.

The XPS spectra of Ga 2*p* in GaN and $Al_{0.7}Ga_{0.3}$ N are shown in Fig. 4b and c, respectively. The main difference between these spectra is the shift of higher binding energy (BE) in the AlGaN film compared to that of the GaN film. It is known that their order of BE is Ga–Ga < Ga–N < Ga–O in Ga 2*p* spectrum. Ga–Al and Ga–Al–N bonds were not found in the spectra obtained from the samples as well as the literature. Using the peak deconvolution of Ga $2p_{3/2}$, the chemical shift is attributed to the appearance of Ga–Ga bond (1116.9 eV), as seen in Fig. 4b. BEs of Ga–N and Ga–O are found to be 1117.9 eV and 1118.5 eV for GaN (1118.6 eV and 1120.0 eV for AlGaN), while the reported BEs of Ga–Ga, Ga–N, and Ga–O are 1116.7, 1117.6–1118.2, and 1120 eV, respectively [19, 20, 26, 27]. Therefore, the BE of Ga 2*p* in the AlGaN film shifted to higher energy owing to the shift of Ga–N and Ga–O in addition to the disappearance of elemental Ga bond. Considering the results of the XPS of nitride films and the J–E characteristics of nitride devices, it

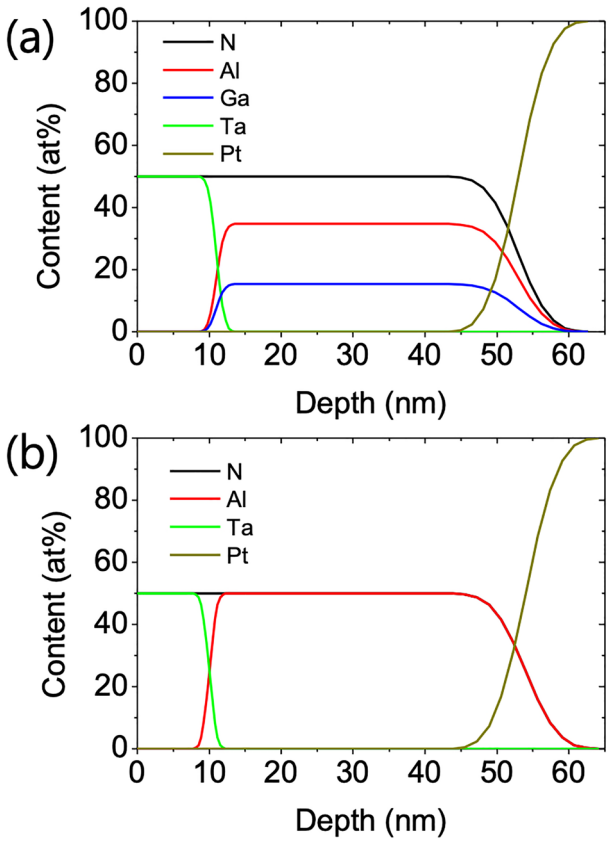

Fig. 3 Elemental composition of **a** AlGaN and **b** AlN films analyzed by Rutherford backscattering spectrometry (RBS)

is concluded that the lower conductivity of the device with $Al_{0.7}Ga_{0.3}$ N was affected by the chemical shift of BEs as well as the contribution of the resistive AlN film itself.

According to a previous study, it was revealed that a significant amount of the upper AlN layer was turned into an oxynitride (AlO_xN_y) during electrical operation due to the intermixing of nitrogen in AlN and oxygen in the top interfacial layer [13]. Such a replacement of nitrogen with oxygen may accelerate the formation of an Al-rich conducting channel in the AlN matrix owing to the ejection of mobile nitrogen ions. Accordingly, a plausible switching mechanism for the AlN memristor was proposed, where the AlN/Pt bottom interface was the active switching interface, and the motion of nitrogen vacancies (V_N^{3+}) was responsible for the switching [12, 13].

To analyse the microstructure of the AlGaN film in the device, cross-sectioning was performed at the electrically deformed location using a focused ion beam (FIB) for $Al_{0.7}Ga_{0.3}$ N memristors. The AlGaN memristor did not show a dramatic change after electroforming and resistive switching, as shown in Fig. 5a. The magnified TEM image in Fig. 5b shows that the AlGaN film was finely crystallized with an average grain size of ~ 2 nm. Energy-dispersive spectroscopy (EDS) mapping in the inset of Fig. 5c shows that both Al and Ga were uniformly distributed in the AlGaN film. Therefore, it is considered that the semiconducting GaN phases are finely distributed and can serve as the precursors of conduction channels, thus simplifying the formation of these channels and leading to the observed high linearity and repeatability. A plausible switching mechanism is illustrated in Fig. 5d. It is considered that AlGaN film is composed of the random mixture of pseudo-binary phase of $(AlN)_x(GaN)_{1-x}$, where insulating AlN and semiconducting GaN are coexisted. This is comparable to the uniformly dispersed Pt nanoparticles with ~ 2-nm-diameter embedded in SiO_2 matrix known as nanometallic resistance switch [28]. Enlarged Pt nanoparticles with the aid of oxygen vacancies in SiO_2 matrix could be involved in the formation of conduction channels owing to the combination of a high electric field and temperature in Pt-SiO_2 system. Similarly,

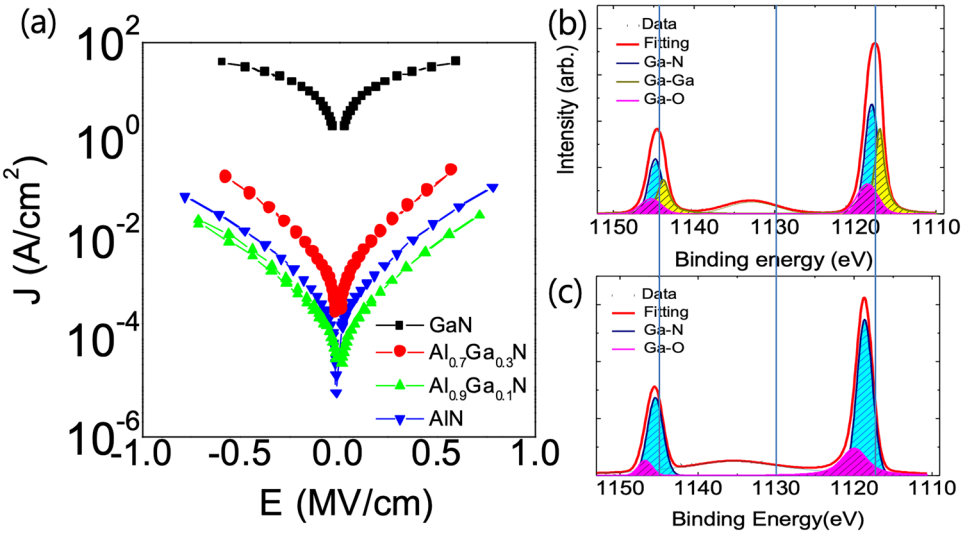

Fig. 4 **a** *J–E* curves of various nitride devices in their initial state. XPS spectra of Ga 2*p* in **b** GaN and **c** $Al_{0.7}Ga_{0.3}$ N films

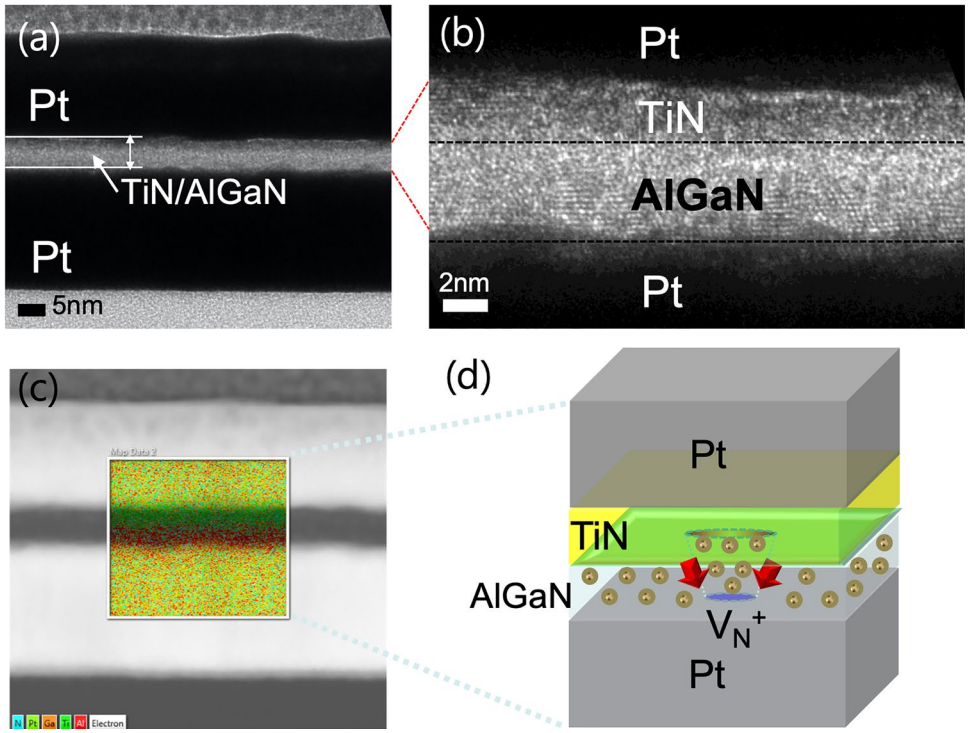

Fig. 5 **a** Low resolution and **b** high resolution cross-sectional TEM images of AlGaN memristor. **c** STEM-EDS mapping and **d** schematic of a plausible switching mechanism of AlGaN memristor

semiconducting GaN phases are uniformly distributed in the insulating AlN matrix in AlGaN alloying film, then nitrogen vacancies may form the conduction channel in between the GaN phases. The nonlinearity of the AlN memristor might be the result of AlO_xN_y formation in the top interfacial layer [13]. However, in the case of the AlGaN memristor, a uniformly distributed GaN phase may hinder excessive heating and formation of an interfacial layer at the top.

4 Conclusion

Ternary nitride memristors made of TiN/AlGaN/Pt were fabricated and characterized in this study. Highly linear and repeatable resistive switching was observed in AlGaN memristors in terms of resistance and switching voltage. Structural and chemical analyses revealed that finely distributed semiconducting GaN phases are attributed to more uniform resistive switching in AlGaN memristors due to the formation of conduction channels with low variability. This novel nitride memristor could be incredibly useful in realizing an analog synaptic device as a neuromorphic computing element as well as nonvolatile memory applications.

Acknowledgements This research was supported by the MOTIE (Ministry of Trade, Industry & Energy (10080625)) and KSRC (Korea Semiconductor Research Consortium) support program for the development of the future semiconductor device. This work has supported by the National Research Foundation of Korea (NRF) grant funded by the Korea government (MSIT) (NRF-2020R1F1A1076232).

References

1. K. Roy, A. Jaiswal, P. Panda, Nat. **575**, 607 (2019)
2. M.A. Zidan, J.P. Strachan, W.D. Lu, Nat. Electron. **1**, 22 (2018)
3. Z. Wang, H. Wu, G.W. Burr, C.S. Hwang, K.L. Wang, Q. Xia, J.J. Yang, Nat. Rev. Mater. **5**, 173 (2020)
4. D.S. Jeong, K.M. Kim, S. Kim, B.J. Choi, C.S. Hwang, Adv. Electron. Mater. **2**, 1600090 (2016)
5. C. Li, M. Hu, Y. Li, H. Jiang, N. Ge, E. Montgomery, J. Zhang, W. Song, N. Dávila, C.E. Graves, Z. Li, J.P. Strachan, P. Lin, Z. Wang, M. Barnell, Q. Wu, R.S. Williams, J.J. Yang, Q. Xia, Nat. Electron. **1**, 52 (2018)
6. M. Hu, C.E. Graves, C. Li, Y. Li, N. Ge, E. Montgomery, N. Davila, H. Jiang, R.S. Williams, J.J. Yang, Q. Xia, J.P. Strachan, Adv. Mater. **30**, 1705914 (2018)
7. Z. Sun, G. Pedretti, A. Bricalli, D. Ielmini, Sci. Adv. **6**, eaay2378 (2020)
8. S. Choi, Y. Kim, T. Van, W.H. Jeong, K.-S. Min, B.J. Choi, Adv. Electron. Mater. **7**, 2100050 (2021)
9. V.K. Sangwan, M.C. Hersam, Nat. Nanotechnol. **15**, 517 (2020)
10. Q. Xia, J.J. Yang, Nat. Mater. **18**, 309 (2019)
11. D.S. Jeong, C.S. Hwang, Adv. Mater. **30**, 1704729 (2018)
12. B.J. Choi, J.J. Yang, M.X. Zhang, K.J. Norris, D.A.A. Ohlberg, N.P. Kobayashi, G. Medeiros-Ribeiro, R.S. Williams, Appl. Phys. A: Mater. Sci. Proc. **109**, 1 (2012)
13. B.J. Choi, A.C. Torrezan, J.P. Strachan, P.G. Kotula, A.J. Lohn, M.J. Marinella, Z. Li, R.S. Williams, J.J. Yang, Adv. Func. Mater. **26**, 5290 (2016)
14. S. Kim, Y.F. Chang, M.H. Kim, T.H. Kim, Y. Kim, B.G. Park, Materials **10**, 459 (2017)
15. D.S. Jeon, J.H. Park, M.J. Kim, T.G. Kim, Appl. Phys. Lett. **109**, 183507 (2016)
16. Q. Zhou, Q. Lu, Y. Zhou, Y. Yang, X. Du, X. Zhang, X. Wu, Surf. Coat. Technol. **229**, 135 (2013)

17. B.J. Murdoch, D.G. McCulloch, R. Ganesan, D.R. McKenzie, M.M.M. Bilek, J.G. Partridge, Appl. Phys. Lett. **108**, 143504 (2016)
18. Y. Guo, W. Hu, C. Zhang, Y. Peng, Y. Guo, J. Phys. D: Appl. Phys. **53**, 195101 (2020)
19. H. Kim, S. Choi, B.J. Choi, Coatings **10**, 489 (2020)
20. S. Choi, A.S. Ansari, H.J. Yun, H. Kim, B. Shong, B.J. Choi, J. Alloy Compd. **854**, 157186 (2020)
21. C. Ozgit-Akgun, E. Goldenberg, A.K. Okyay, N. Biyikli, J. Mater. Chem. C **2**, 2123 (2014)
22. Y. Kim, M.S. Kim, H.J. Yun, S.Y. Ryu, B.J. Choi, Ceram. Inter. **44**, 17447 (2018)
23. M. Monish, S. Mohan, D.S. Sutar, S.S. Major, Semicon. Sci. Technol. **35**, 045011 (2020)
24. K. Ueno, F. Taiga, A. Kobayashi, H. Fujioka, Sci. Rep. **9**, 20242 (2019)
25. N. Nepal, J. Li, M.L. Nakarmi, J.Y. Lin, H.X. Jiang, Appl. Phys. Lett. **87**, 242104 (2005)
26. M. Alevli, A. Haider, S. Kizir, S.A. Leghari, N. Biyikli, J. Vac. Sci. Technol. A **34**, 01A137 (2015)
27. P. Motamedi, K. Cadien, Appl. Surf. Sci. **315**, 104 (2014)
28. B.J. Choi, A.C. Torrezan, K.J. Norris, F. Miao, J.P. Strachan, M.X. Zhang, D.A.A. Ohlberg, N.P. Kobayashi, J.J. Yang, R.S. Williams, Nano Lett. **13**, 3213 (2013)